Air Qual Atmos Health (2018) 11:95–109
https://doi.org/10.1007/s11869-017-0523-7

Spatial and temporal variations in criteria air pollutants in three typical terrain regions in Shaanxi, China, during 2015

Yong Xu[1] · Qi Ying[2,3] · Jianlin Hu[3] · Yuan Gao[1] · Yang Yang[1] · Dexiang Wang[1] · Hongliang Zhang[3,4]

Received: 17 July 2017 / Accepted: 6 October 2017 / Published online: 23 October 2017

Abstract Numerous studies have investigated air pollution in severely polluted plains, but the characteristics of pollutants are not well understood in other terrain regions. In this study, air pollution characteristics were analyzed in three typical terrain regions (plateau, plain, and mountain regions) in Shaanxi, based on hourly ambient monitoring of particulate matter with diameter less than 2.5 μm ($PM_{2.5}$) and less than 10 μm (PM_{10}), CO, SO_2, NO_2, and O_3 in 2015. $PM_{2.5}$ and PM_{10} were the dominant pollutants in three regions, and their annual concentrations exceeded the Grade II standards by 9.4–68.6 and 6.0–73.9%, respectively. $PM_{2.5}$, PM_{10}, CO, SO_2, and NO_2 concentrations had similar seasonal trends with highest values in winter and lowest values in summer, whereas O_3 concentrations exhibited the opposite trend. Guanzhong Plain had higher $PM_{2.5}$, PM_{10}, NO_2, and SO_2 concentrations but lower CO, 1-h peak O_3, and 8-h peak O_3 (8 h-O_3) compared to other regions. $PM_{2.5}$, PM_{10}, and 8 h-O_3 were the three main dominant pollutants. The nonattainment rate was highest in winter and lowest in summer or autumn. Pollution also exhibited synergy, especially in the plateau region and Guanzhong Plain. $PM_{2.5}$ was significantly correlated with PM_{10}. NO_2 and SO_2 were positively correlated with $PM_{2.5}$ and PM_{10}, while 8 h-O_3 generally had significant negative correlations with other pollutants, especially in the winter. These results provide a comprehensive understanding of pollution status in the three typical terrain regions in Shaanxi and are helpful for improving air quality.

Keywords Air pollutant · Terrain region · Guanzhong · Spatial variation · Temporal variation

Electronic supplementary material The online version of this article (https://doi.org/10.1007/s11869-017-0523-7) contains supplementary material, which is available to authorized users.

✉ Dexiang Wang
wangdx66@126.com; wangdx66@sohu.com

✉ Hongliang Zhang
hlzhang@lsu.edu

[1] College of Forestry, Northwest A&F University, Yangling, Shaanxi 712100, China

[2] Department of Civil Engineering, Texas A&M University, College Station, TX 77843, USA

[3] Jiangsu Key Laboratory of Atmospheric Environment Monitoring and Pollution Control, Jiangsu Engineering Technology Research Center of Environmental Cleaning Materials, Collaborative Innovation Center of Atmospheric Environment and Equipment Technology, School of Environmental Science and Engineering, Nanjing University of Information Science and Technology, 219 Ningliu Road, Nanjing 210044, China

[4] Department of Civil and Environmental Engineering, Louisiana State University, Baton Rouge, LA 70803, USA

Introduction

China has experienced severe air pollution due to economic growth in recent years (Guo et al. 2014). Haze has occurred more frequently on a large scale according to satellite observations (http://www.weather.com.cn/air), especially in the winter, thereby suggesting that air pollution is no longer limited to megacities and urban areas. The air pollution levels are determined based on the composition and concentrations of a complex mixture of air pollutants. The main air pollutants emitted into the atmosphere are SO_2, NO_2, CO, volatile organic compounds (VOCs), and particulate matter with diameter less than 2.5 μm ($PM_{2.5}$) and less than 10 μm (PM_{10}). In addition, the reactions between VOC and nitrogen oxides (NO_x) producing O_3 in the planetary boundary layer (PBL) have major effects on human health (Lei et al. 2007; Tie et al. 2007; Zhao et al.

2006). SO_2, NO_2, CO, O_3, $PM_{2.5}$, and PM_{10} are generally defined as criteria air pollutants for quantifying air pollution levels. These pollutants are investigated to evaluate the air quality, pollution formation/transport mechanisms, health risks, and to assess the effectiveness of proposed air pollution control measures (Gurjar et al. 2008; Hu et al. 2015; Wang et al. 2014b; Wang et al. 2014c; Zhang et al. 2004).

The Ministry of Environmental Protection of China (MEP) started publishing daily air pollution index (API) data for a number of key cities in 2000 (increasing from 47 cities in 2000 to 120 cities in 2011) based on ground monitoring of the 24-h average concentrations of SO_2, NO_2, and PM_{10} (http://datacenter.mep.gov.cn/index). Thus, studies based on monitoring data before 2011 were restricted to the values obtained for API, SO_2, NO_2, and PM_{10} (Gao et al. 2011; Qu et al. 2010; Ji et al. 2012). The monitoring of $PM_{2.5}$ and O_3 was not required as per Chinese Ambient Air Quality Standards (CAAQS) guidelines until February 2012 when the third revision of the Chinese Ambient Air Quality Standards GB 3095–2012 (CAAQS) (http://kjs.mep.gov.cn/hjbhbz/bzwb/dqhjbh/dqhjzlbz/201203/W020120410330232398521.pdf) was released. In addition, the MEP also released an official revision of the ambient air quality index (AQI), which was calculated based on the values observed for six criteria pollutants comprising SO_2, NO_2, $PM_{2.5}$, PM_{10}, CO, 1-h peak O_3 (1 h-O_3), and 8-h peak O_3 (8 h-O_3) in March 2012. Subsequently, more cities (from 76 cities in 2013 to 367 cities in 2015 after many less-developed cities were added) began to release the concentrations of these six criteria pollutants and the calculated AQI values to the public (http://datacenter.mep.gov.cn/index). Using this rich dataset, it is possible to perform comprehensive evaluations of the air quality at a fine spatial scale.

Characteristics of criteria pollutants have been analysis in different areas of China. For example, Chai et al. (2014) determined the spatial and temporal variations of the six criteria pollutants in 16 Chinese provincial cities using data collected between August 2011 and February 2012. Hourly monitoring data for the six pollutants in 31 provincial capital cities in China from March 2013 to February 2014 were analyzed by Wang et al. (2014b) and Zhao et al. (2016). Temporal and spatial variations in PM also were investigated with fine precision at the city scale (Hu et al. 2014; Zhang and Cao 2015). Most studies only focused on the spatial and temporal variations of a few pollutants in provincial cities throughout China, so the spatial scale was relatively coarse and the pollution characteristics at city scale for less-developed provinces containing different terrains have not been comprehensively studied.

Shaanxi is a major province in northwest China, which has the three type terrains from north to south (plateau, plain, and mountains regions), and previous studies of this region have focused mainly on limited pollutants in the Guanzhong area, especially Xi'an (Qu et al. 2010; Wang et al. 2014a; Zhang et al. 2016; Zhao et al. 2016). Thus, this study aimed to investigate the temporal and spatial variations of criteria air pollutants, the air quality attainment status, major pollutants, correlations among cities for each pollutant, and regional relationships among pollutants based on 1-year monitoring data at the city scale in the three typical terrain regions in Shaanxi.

Methods and data

Study domain

The study area of Shaanxi ranges from 105° 29′ E to 111° 15′ E and 31° 42′ N to 39° 35′ N, and it contains ten administrative cities (Fig. 1). The topography is complex, and it can be divided into three types from north to south, i.e., the Loess Plateau in the north including Yulin and Yan'an; the Guanzhong Plain in the middle including Baoji, Xi'an, Xianyang, Tongchuan, and Weinan; and the Qinba Mountains region in the south including Hanzhong, Ankang, and Shangluo. The north–south climate is divided by the Qinling Mountains and precipitation plays an important role in determining the two climates. Thus, humid, semi-humid, and semiarid areas are categorized according to the three topographies from south to north. In general, the spring is warm and dry with less precipitation, while the temperature is changeable and it increases quickly. The summer is hot and rainy with occasional droughts. The autumn is cool and wet, and the winter is cold and dry with rare rain and snow. To evaluate the annual and seasonal air quality in each city in the three terrains in Shaanxi, we analyzed ambient monitoring data for $PM_{2.5}$, PM_{10}, CO, SO_2, NO_2, 1 h-O_3, and 8 h-O_3 during 2015 for the whole year. Ten cities were categorized into three general regions, i.e., plateau, Guanzhong plain, and Mountain representing the Loess Plateau, Guanzhong Plain, and Qinba Mountains regions, respectively. The population, number of vehicles, and gross domestic product for each city are listed in Table 1.

Data collection

Real-time hourly observation data for $PM_{2.5}$, PM_{10}, CO, SO_2, NO_2, and O_3 at each monitoring site in the ten cities were downloaded from the website of the China National Environmental Monitoring Center (http://113.108.142.147:20035/emcpublish/). Multiple national air quality monitoring sites (2–13) are present in each city, with most in urban areas and a few in suburban areas (Fig. 1). The SO_2, NO_2, O_3, and CO measurements were determined according to China Environmental Protection Standards HJ 193–2013 (http://www.es.org.cn/download/2013/7–12/2627–1.pdf),

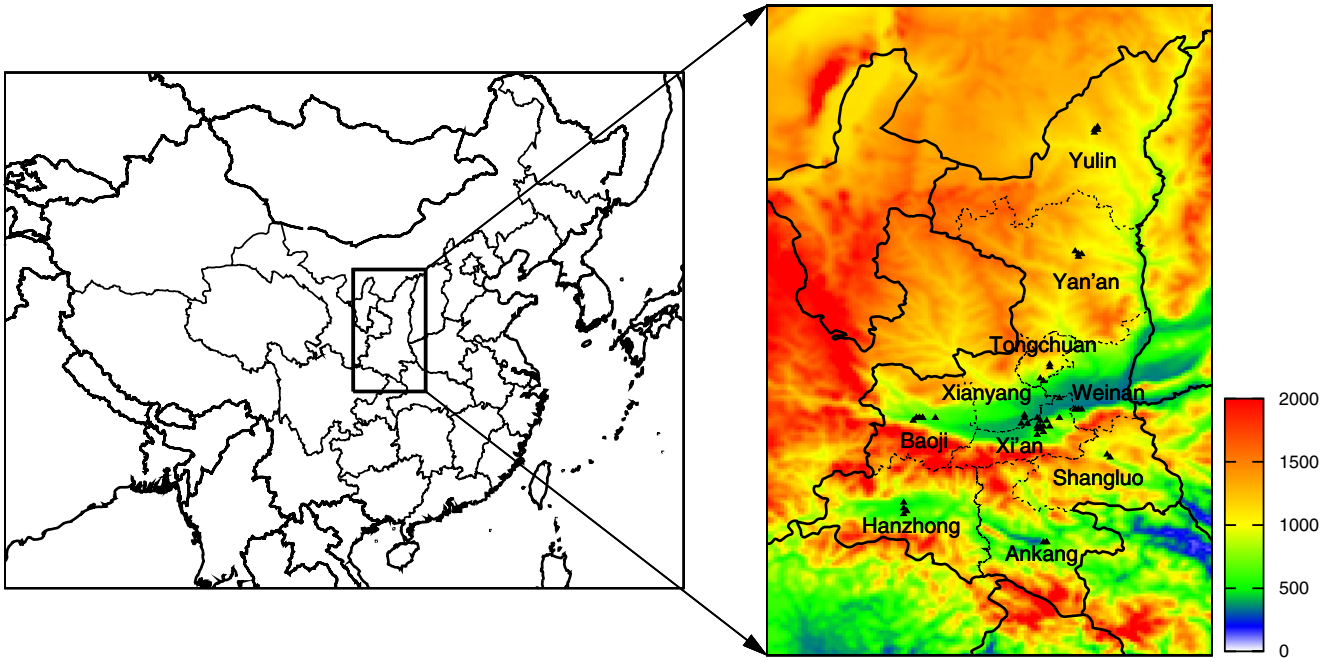

Fig. 1 Geographical location of Shaanxi, terrain elevation, and locations of air quality monitoring sites. The colour shows the elevation height and black triangles repesent the locations of air quality monitoring sites in each city

and those for $PM_{2.5}$ and PM_{10} were obtained according to China Environmental Protection Standards HJ 655–2013 (http://www.es.org.cn/download/2013/7–12/2626–1.pdf).

SO_2, NO_2, and O_3 are measured by the ultraviolet fluorescence method (TEI, Model 43i from Thermo Fisher Scientific Inc., USA, or EC9850 from Ecotech Pty Ltd., Australia), the chemiluminescence method (TEI Model 42i from Thermo Fisher Scientific Inc., USA, or EC9841 from Ecotech Pty Ltd., Australia), and the UV-spectrophotometry method (TEI model 49i from Thermo Fisher Scientific Inc., USA, or EC9810 from Ecotech Pty Ltd., Australia), respectively. CO is measured using the nondispersive infrared absorption method and the gas filter correlation infrared absorption method (API Model 300 from Teledyne Advanced Pollution Instrumentation, USA, or TEI, Model 48i from Thermo Fisher Scientific Inc., USA, or EC9830 from Ecotech Pty Ltd., Australia). The microoscillating balance method (TEOM from Rupprecht & Patashnick Co., Inc., USA) and the β absorption method (BAM 1020 from Met One Instrument Inc., USA or Tianhong Co., China or Xianhe Co., China) are used to measure $PM_{2.5}$ and PM_{10}. The concentrations of the gases and aerosols are relatively high during the study period and are always higher than the minimal detection limit of the instruments. The details of the methods were explained by Zhao et al. (2016). The values were automatically uploaded to the NEM and published after validation according

Table 1 Region category, population, vehicle numbers, gross domestic product (GDP), and number of nonattainment days in the ten cities in Shaanxi during 2015

City	Region category	Population (million)	Vehicle numbers (thousand)	GDP (billion yuan)	Number of nonattainment days (for standard II)	Number of nonattainment days (for standard I)	Number of valid days
Yulin (YL)	Plateau	3.38	510	262.1	71	336	362
Yan'an (YA)	Plateau	2.21	246	119.9	73	346	362
Baoji (BJ)	Plain	3.75	205	178.9	86	339	362
Xi'an (XA)	Plain	8.63	1966	581.0	96	342	362
Xianyang (XY)	Plain	5.05	271	215.6	93	337	362
Tongchuan (TC)	Plain	0.85	69	32.5	92	341	362
Weinan (WN)	Plain	5.34	394	146.9	92	342	362
Ankang (AK)	Mountain	2.64	94	77.2	66	286	362
Hanzhong (HZ)	Mountain	3.43	174	99.1	71	282	362
Shangluo (SL)	Mountain	2.35	67	62.2	50	321	356

Source: http://www.shaanxitj.gov.cn/site/1/html/126/132/142/list.htm

to the Technical Guideline on Environmental Monitoring Quality Management HJ 630–2011(http://kjs.mep.gov.cn/hjbhbz/bzwb/other/qt/201109/W020120130585014685198.pdf). The hourly data were subjected to a sanity check in order to remove any problematic data points according to CAAQS, as described by Zhao et al. (2016).

In order evaluate the effect of meteorology on pollutants, temperature, relative humidity, and wind speed was downloaded from NOAA's National Climatic Data Center (ftp://ftp.ncdc.noaa.gov/pub/data/noaa/2015) and the daily data of atmospheric pressure, temperature, relative humidity, wind speed, and sunshine hours were obtained from the National Daily Surface Climate Dataset (V3.0) (http://data.cma.cn/data/cdcdetail/dataCode/SURF_CLI_CHN_MUL_DAY_CES_V3.0.html), which was prepared by the National Meteorological Information Center from the automatic uploaded hourly surface monitoring data.

Analytical methods

The daily concentrations at each site were calculated only when 18 valid hourly values were available for that day. The citywide daily average concentrations of $PM_{2.5}$, PM_{10}, CO, SO_2, and NO_2 were the average values of the corresponding daily average concentrations at all monitoring sites in each city. The citywide average hourly concentrations were calculated when valid hourly data for the corresponding pollutant were available for more than two thirds of the monitoring sites. The daily 8 h-O_3 concentrations were calculated based on the average diurnal O_3 concentrations when valid data were available for at least 6 h out of every 8 h, and the maximum value was selected among all the calculations. The daily 1 h-O_3 concentration was the maximum value among the valid diurnal data. The citywide seasonal average values were calculated by averaging the citywide daily average values, with a requirement for more than 81 values during each season. Similarly, the citywide annual average values were also calculated based on the citywide daily average values, with a requirement for more than 324. The citywide daily, seasonal, and annual average concentrations of $PM_{2.5}$, PM_{10}, CO, SO_2, and NO_2, as well as the 1 h-O_3 and 8 h-O_3 concentrations were calculated according to these principles. The same dataset and method were also used in previous studies (Hu et al. 2014; Wang et al. 2014c). The days when the daily average concentrations of at least one pollutant exceeded the CAAQS Grade II standard were defined as nonattainment days.

Correlation coefficients were calculated to analyze the possible synergy among pollutants, and the interregional relationships among pollutants were determined based on the daily average concentrations. To assess the diurnal variations in $PM_{2.5}$, PM_{10}, CO, SO_2, NO_2, and O_3, the citywide seasonal diurnal concentrations were determined when more than 81 of the corresponding citywide hourly average values for each hour were available in each season. Similarly, the citywide annual diurnal values were calculation based on the corresponding citywide hourly average values, with a requirement for more than 324. Additionally, the average diurnal variations in temperature, relative humility, and wind speed in four seasons and annual and seasonal average values of atmospheric pressure, temperature, relative humility, wind speed, and sunshine hours were also calculated. Besides, 72-h air mass backward trajectory analysis (Rolph et al. 2017; Yerramilli et al. 2012) was conducted in the most polluted 11 consecutive days in each cities in the four seasons using NOAA HYSPLIT Model (http://ready.arl.noaa.gov/HYSPLIT.php) to understand the seasonal variations in inter- and extra-regional pollutions among different terrain regions in Shaanxi.

Results and discussion

Overall air pollutant concentrations

The annual average concentrations of the six pollutants were calculated for the ten cities (Table 2). The ten cities experienced air pollution where the daily average concentrations of at least one pollutant exceeded the CAAQS Grade I standard on more than 2 out of 3 days, and the CAAQS Grade II standard was exceeded on 16–28% of the total days in 2015. All ten cities were affected by severe particulate matter pollution.

The annual average concentration of $PM_{2.5}$ ranged from 38.3 μg/m^3 (Yulin) to 59.0 μg/m^3 (Xianyang), thereby exceeding the corresponding Grade II standard (35 μg/m^3) by 9.4–68.6%, and PM_{10} ranged from 74.2 μg/m^3 (Ankang) to 121.7 μg/m^3 (Xi'an), which exceeded the corresponding Grade II standard (70 μg/m^3) by 6.0–73.9% (Table 2). SO_2 ranged from 4.9 ppb (Hanzhong) to 8.6 ppb (Yan'an), where seven cities exceeded the Grade I standard (20 μg/m^3, ~ 7 ppb), excluding Yulin, Baoji, and Hanzhong, but no cities exceeded the Grade II standard (60 μg/m^3, ~ 21 ppb). NO_2 ranged from 8.3 ppb (Ankang) to 20.7 ppb (Yan'an), and only Xi'an and Yan'an exceeded the Grade I and II standards (40 μg/m^3, ~ 19.5 ppb). The CO concentration ranged from 0.9 ppm (Weinan) to 1.42 ppm (Yan'an). The annual average 1 h-O_3 concentration ranged from 41.0 ppb (Xianyang) to 51.9 ppb (Shangluo), and the 8 h-O_3 concentration ranged from 33.8 ppb (Xianyang) to 45.3 ppb (Shangluo). Daily average CO, 1 h-O_3, and 8 h-O_3 standards are defined in CAAQS, but CO, 1 h-O_3, and 8 h-O_3 annual standards are not defined in CAAQS for evaluating the annual concentrations of CO and O_3 in these cities.

The annual and seasonal distributions of the pollutant concentrations in the ten cities are shown in Figs. 2 and 3. In terms of their temporal distributions, the concentrations of $PM_{2.5}$, PM_{10}, CO, SO_2, and NO_2 all exhibited similar seasonal trends,

Table 2 Annual average concentrations of the criteria air pollutants in the ten cities in Shaanxi

	$PM_{2.5}$ (μg/m^3)	PM_{10} (μg/m^3)	CO (ppm)	SO_2 (ppb)	NO_2 (ppb)	1 h-O_3 (ppb)	8 h-O_3 (ppb)
Yulin (YL)	38.3 ± 23.5	86.6 ± 46.4	1.37 ± 0.77	6.5 ± 4.7	17.3 ± 7.2	51.5 ± 17.3	45.1 ± 17.1
Yan'an (YA)	45.1 ± 24.0	99.8 ± 42.0	1.42 ± 0.74	8.6 ± 8.3	20.7 ± 5.3	50.5 ± 18.5	42.7 ± 18.0
Baoji (BJ)	56.1 ± 42.3	105.7 ± 61.2	1.10 ± 0.49	5.0 ± 3.6	16.8 ± 5.6	41.9 ± 20.7	34.8 ± 18.7
Xi'an (Querol et al.)	56.7 ± 38.3	121.7 ± 67.7	1.30 ± 0.54	8.5 ± 5.0	19.5 ± 6.9	42.8 ± 23.2	34.8 ± 19.9
Xianyang (XY)	59.0 ± 44.3	112.4 ± 66.1	0.99 ± 0.40	8.0 ± 4.5	18.1 ± 7.5	41.0 ± 20.2	33.8 ± 17.6
Tongchuan (TC)	55.3 ± 38.5	103.6 ± 52.6	0.96 ± 0.44	8.3 ± 6.9	16.5 ± 6.3	47.5 ± 17.3	40.6 ± 16.2
Weinan (WN)	58.7 ± 49.0	111.9 ± 72.9	0.90 ± 0.50	8.0 ± 4.8	19.3 ± 7.5	44.3 ± 21.1	36.8 ± 18.6
Ankang (AK)	50.0 ± 35.7	74.2 ± 46.5	0.92 ± 0.44	8.3 ± 4.7	8.3 ± 4.6	46.6 ± 17.1	39.7 ± 16.0
Hanzhong (HZ)	53.5 ± 39.9	76.9 ± 46.9	1.03 ± 0.46	4.9 ± 2.6	12.8 ± 5.3	45.2 ± 18.8	37.4 ± 17.0
Shangluo (SL)	43.2 ± 27.3	76.5 ± 45.7	1.38 ± 0.53	8.0 ± 5.0	12.5 ± 4.4	51. 9 ± 15.8	45.3 ± 15.2

with the highest levels in the winter and the lowest in the summer, while there were intermediate concentrations in the spring and autumn, with little difference among all three regions. The high concentrations of pollutants in the winter were caused directly by large increases in coal combustion and the burning of biomass or biofuel for heating. In addition, temperature inversion, and the highest atmospheric pressure (Table S1) causing low PBL height allowed pollutants to accumulate in a shallow layer with descending air motions (Ji et al. 2012). By contrast, in the summer, the temperature was high with low atmospheric pressure (Table S1), the usually unstable state was beneficial for dispersing pollutants, and heavy precipitation also removed pollutants, thereby leading to low concentrations. However, the 8 h-O_3 and 1 h-O_3 concentrations exhibited the opposite seasonal trends compared with the other pollutants.

In terms of their spatial distributions, the concentrations of $PM_{2.5}$, PM_{10}, NO_2, and SO_2 in Guanzhong Plain cities were usually higher than those in other two regions, whereas those of CO, 1 h-O_3, and 8 h-O_3 were lower. In general, the spatial distributions of pollutants are influenced greatly by local sources. Guanzhong Plain was the most developed region with the highest GDP (Table 1), where coal-fired power plants and industries with large units, including factories producing cement, chemicals, and metals, were mainly concentrated in 2015 (Fig. S1). Furthermore, due to the surrounding high mountains, there is a lack of air movement and the air mass encounter obstacles when moving out from the plain (Jazcilevich et al. 2005). However, the 8 h-O_3 concentrations exhibited contrasting spatial variations, where they were always slightly higher in the plateau and mountain regions, possibly because of the relatively higher solar radiation with long sunshine hours (Table S1) and lower NO_2 concentrations (Fig. 3), respectively.

Variations in species

The detailed spatial variations in the concentration of each pollutant among the three regions during the four seasons were compared to determine their spatial and temporal differences. The annual concentration of $PM_{2.5}$ followed the order of Guanzhong Plain > mountain region > plateau region. There were almost no differences among the ten cities in the three regions during the spring and summer. In the autumn, the concentrations in Guanzhong Plain were slightly higher than those in the other two regions, which had similar concentrations. In the winter, the concentrations were lowest in the plateau region, while the concentrations in the mountain region (except Shangluo) were similar to those in Guanzhong Plain. The air mass trajectory analysis of the cities in the two terrain regions when $PM_{2.5}$ concentration was high in winter (Fig. S2) showed that the two regions had interregional transport in the winter, and the frequent short trajectory also indicated that pollutants were retained easily in the mountain region (except Shangluo). In addition, poor meteorological conditions with less rainfall and poor restricted in the south contributed to the increased concentration (Gao et al. 2011). However, Shangluo is in a valley toward the northwest along the path of the winter monsoon and the wind speed was relatively high (two times of that in Ankang and Hanzhong) (Table S1), which favors the dispersion of pollutants. The concentration of PM_{10} was also highest in Guanzhong Plain (Fig. 2). However, the concentration of PM_{10} was higher in the plateau region than the mountain region, except during the winter, which contrasted with the trends in $PM_{2.5}$. This difference occurred because there is a source of suspended particulate matter in the plateau region during dry and windy weather as the Loess Plateau is arid and much of its surface is exposed (Zhang et al. 2002; Zhao et al. 2006), especially during the spring when dusty weather occurs(Wang et al. 2014c; Yang et al. 2011). Back-trajectory analysis for the two cities when PM_{10} concentration was high in spring showed dust transported by the strong winds from the Mongolia can be a significant contributor (Fig. S2). Furthermore, the number of industries was much lower in the mountain region, and thus, they produced less PM_{10}. The ratios of $PM_{2.5}$ relative to that of PM_{10} in the four seasons was in the order of mountain region

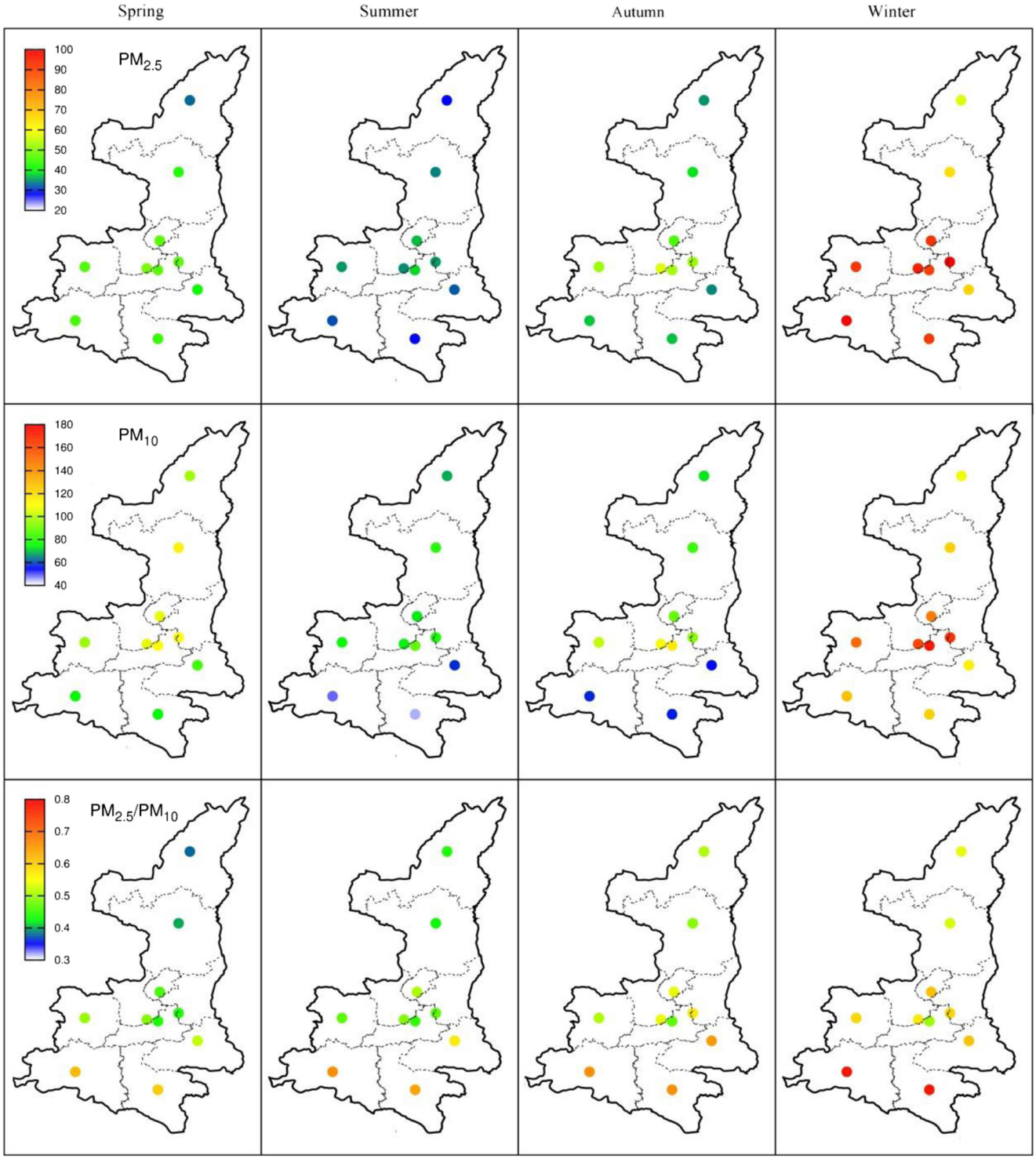

Fig. 2 Seasonal concentrations of $PM_{2.5}$ and PM_{10} (in $\mu g/m^3$) as well as the $PM_{2.5}/PM_{10}$ ratios

> Guanzhong Plain > plateau region, corresponding to the seasonal PM_{10} and $PM_{2.5}$ orders. The cities with relatively lower $PM_{2.5}/PM_{10}$ ratios in the plateau region were likely having more primary PM sources, such as PM_{10} from dust. The ratios in the mountain region were highest did reflect there were less PM emissions sources, and the frequent short back-trajectory lines indicated the longtime for the formation of second $PM_{2.5}$ (Fig. S2). The ratio increased from the spring to winter in all regions, as the $PM_{2.5}/PM_{10}$ ratio increased during high PM events (Hu et al. 2014). The ratios in the three regions were all larger than 0.5 in the winter, partly because the poor meteorology were responsible for the weak dilution

of primary pollutants and enhanced secondary PM formation, e.g., the conversion rates of NO_x and SO_2 from the gas phase to the particle phases of NO_3 and SO_4 were higher (Quan et al. 2014). The substantial fraction of PM_{10} mass was in the $PM_{2.5}$ size range suggests that $PM_{2.5}$ control strategies will also be effective in reducing the PM_{10} pollution, especially in the mountain region.

Higher CO concentrations were observed in the plateau region (Fig. 3), which may have been due to the large number of coal-fired power plants and industries in Yulin (Fig. S1). Yan'an is a linear narrow city stretching along a "Y"-type valley, which induces the formation of a local confluence line in the city, thereby accumulating the CO produced mainly by traffic and residents, with high CO concentrations (Jazcilevich et al. 2005). This could also explain why most of the pollutant concentrations in Yan'an were higher than those in Yulin despite the fact that Yulin contained many more industries. Besides, back-trajectory analysis in the two cities showed that although air mass were mainly from northwest regions, Yan'an was more frequently influenced by Yulin and other regions, i.e., Guanzhong Plain and eastern China (Fig. S2). However, although Shangluo had the lowest levels of coal consumption and vehicles, it was unexpectedly affected by severe CO pollution. It has been studied that the concentrations of long-lived pollutants (i.e., CO and SO_2) are influenced significantly by wind, and regional transport is also a major determinant of high CO concentrations (Zhu et al. 2016). The concentration of SO_2 in the mountain region was slightly higher than that in the plateau region during all seasons except the winter (Fig. 3). Unexpectedly, Yan'an had the highest concentration of SO_2 among the ten cities in the winter, which may be attributable to the "Y"-type valley where it is located. The concentrations of NO_2 in the plateau region were similar to those in Guanzhong Plain, but higher than those in the mountain region during all four seasons (Fig. 3). The NO_2 concentration was high in the plateau region because of the many industries present in Yulin and the special urban terrain of Yan'an. The NO_2 was derived mainly from mobile and stationary sources, and the concentrations were low due to the small number of vehicles and industries in the mountain region (Table 1). The concentration of NO_2 was considerably higher than that of SO_2 in all cities, partly because the efficiency of flue gas desulfurization was much higher than that of denitrification in the coal-fired power plants in Shaanxi (Xu et al. 2017).

Nonattainment pollutants

The daily "dominant pollutant" is identified as the pollutant that contributes the most to air quality degradation on nonattainment days. The daily individual air quality index (IAQI) is calculated based on the daily concentration of each criteria pollutant according to Technical Regulation on Ambient Air Quality (HJ 633–2012) (http://kjs.mep.gov.cn/hjbhbz/bzwb/dqhjbh/jcgfffbz/201203/t20120302_224166.htm), where the IAQI is 100 when the corresponding pollutant concentration is equal to the CAAQS Grade II standard. The pollutant with the maximum IAQI is defined as the dominant pollutant on nonattainment days (Cheng et al. 2007). The nonattainment days for standard II in each city are shown in Table 1, and the frequencies of each pollutant as the dominant pollutant on the nonattainment days are also illustrated (Fig. 4). $PM_{2.5}$ was the most frequent dominant pollutant (40–90%), followed by PM_{10} (4–40%) and O_3 (3–23%). The frequency of $PM_{2.5}$ was much higher than that of PM_{10} in the mountain region especially in Ankang and Hanzhong (~ 19 times higher), followed by Guanzhong Plain (0.3–2.9 times higher), whereas the frequencies of both were similar in the plateau region. CO, NO_2, and 1 h-O_3 occurred much less frequently as the dominant pollutants (less than 2%).

In order to illustrate the complexity of air pollution, a "nondominant pollutant" was defined as a nonattainment pollutant (IAQI > 100) but not the dominant pollutant. Based on the number of days for each nonattainment pollutant (Fig. 5), PM_{10} was frequently a nondominant pollutant, especially in Guanzhong Plain (40–60%), followed by the mountain region (30–40%) and plateau region (10–20%). In addition, when PM_{10} was a nondominant pollutant, $PM_{2.5}$ was always the dominant pollutant. During 60–90% of the total days when $PM_{2.5}$ was the dominant pollutant, PM_{10} was a nondominant pollutant in Guanzhong Plain, and the rates were 30–50% in the plateau and mountain regions (Table S2). Furthermore, the days when PM_{10} was a nondominant pollutant were concentrated mostly in the winter, i.e., 80–100% in the plateau and mountain regions, and 60–80% in Guanzhong Plain (Table S2). Therefore, PM_{10} occurred frequently as a nondominant pollutant when $PM_{2.5}$ was the dominant pollutant in Guanzhong Plain (~ 81%), the mountain region (~ 46%), and the plateau region (~ 48%) during the winter on nonattainment days (Table S2). The results showed that all of the cities were also affected by combined pollution with $PM_{2.5}$ and PM_{10} on nonattainment days, especially in Guanzhong Plain during the winter. $PM_{2.5}$, 1 h-O_3, 8 h-O_3, and NO_2 were rarely nondominant pollutants, with rates lower than 6%.

Nonattainment rates

According to the seasonal rates of nonattainment days in each city, the seasonal variations were similar in cities in the same region whereas there were some differences among regions (Fig. 6). Furthermore, the frequencies of different criteria pollutants as the dominant pollutants varied among seasons in the three regions (Table 3).

In general, the worst air quality occurred in all of the cities during the winter, where nonattainment days accounted for

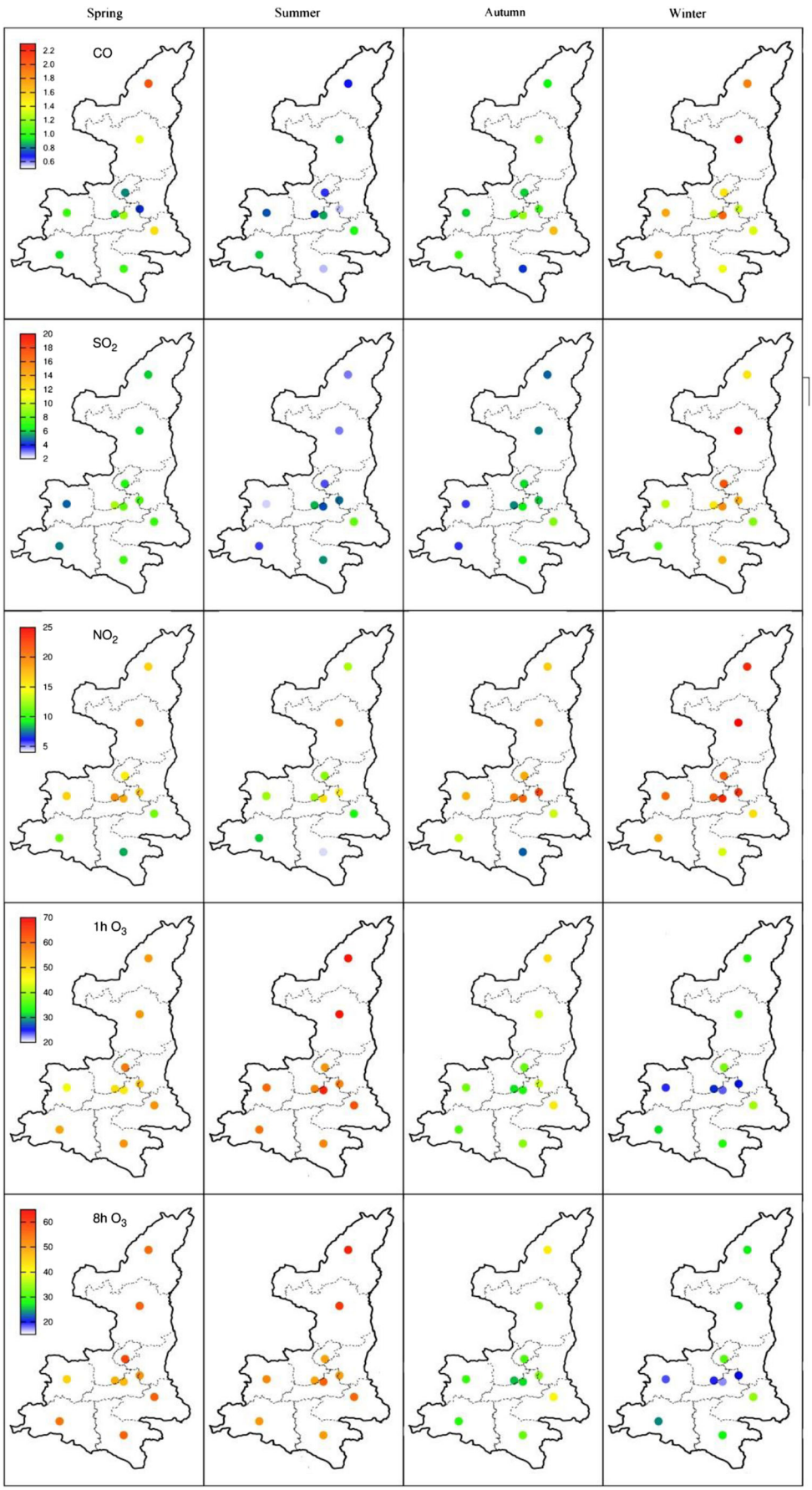

Fig. 3 Seasonal average concentrations of gaseous air pollutants in cities in Shaanxi. The unit is ppm for CO and ppb for other pollutants

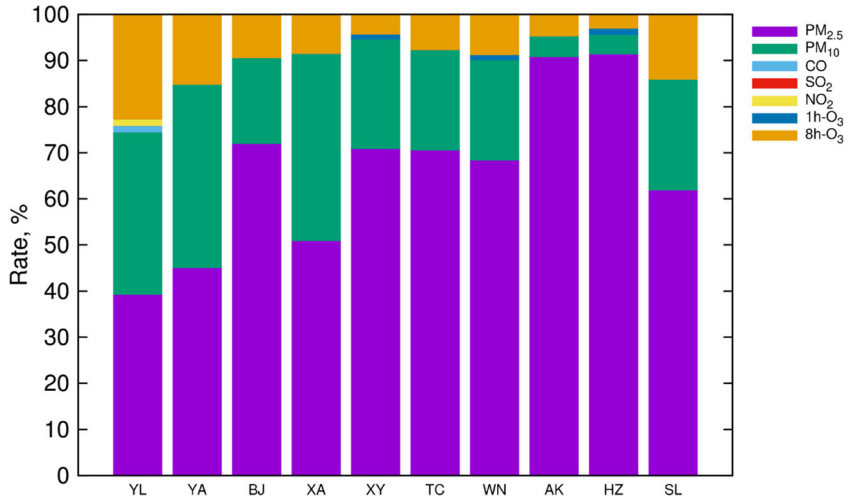

Fig. 4 Frequencies of different pollutants as dominant pollutants on nonattainment days

30–60%. $PM_{2.5}$ was the most frequent dominant pollutant (77–96%), possibly because of increased coal combustion (Ji et al. 2012), and poor meteorological conditions are not conducive to the dispersion of air pollutants in the winter (Gao et al. 2011) as discussed above. During the summer, the nonattainment rate was lowest in the mountain region (~ 3%), where 8 h-O_3 was the most frequent dominant pollutant (> 70%). Similarly, the nonattainment rate was also low in Guanzhong Plain (~ 10%) with comparable frequencies for 8 h-O_3 (~ 51%) and $PM_{2.5}$ (~ 40%) as dominant pollutants. However, the nonattainment rate was not the lowest during the summer in the plateau region where 8 h-O_3 made the greatest contribution (~ 78%) under conditions with high solar radiation (Querol et al. 2014; Santurtún et al. 2015) and long sunshine hours (Table S1). During the autumn, the nonattainment rate was also lowest in the mountain region (~2%). $PM_{2.5}$ was the most frequent dominant pollutant (63–71%), and PM_{10} was the second most frequent (14–38%) in the three regions, but the nonattainment rates were quite different, i.e., ~ 2% in the mountain region, ~ 21% in Guanzhong Plain, and ~ 9% in the plateau region, thereby indicating severe $PM_{2.5}$ pollution in Guanzhong Plain during the autumn. During the spring, the nonattainment rate was ~ 22% in the plateau region where PM_{10} made the main contribution (~ 74%) due to the effects of dusty weather (Wang et al. 2014c; Yang et al. 2011). The contributions of $PM_{2.5}$ (~ 41%) and PM_{10} (~ 48%) to the nonattainment rate (~ 19%) as dominant pollutants were similar in Guanzhong Plain. In the mountain region, $PM_{2.5}$ (~ 54%) and PM_{10} (~ 30%) were the two main dominant pollutants that contributed to the nonattainment rates (~ 13%), and 8 h-O_3 was the third main dominant pollutant, which made similar contributions (12–15%) to the nonattainment rates in the three regions during the spring.

Synergy among pollutants

In general, the concentrations of air pollutants can be influenced greatly by regional transportation within the same region, where the similar geography and meteorology have important effects (Gao et al. 2011; Zhu et al. 2016).

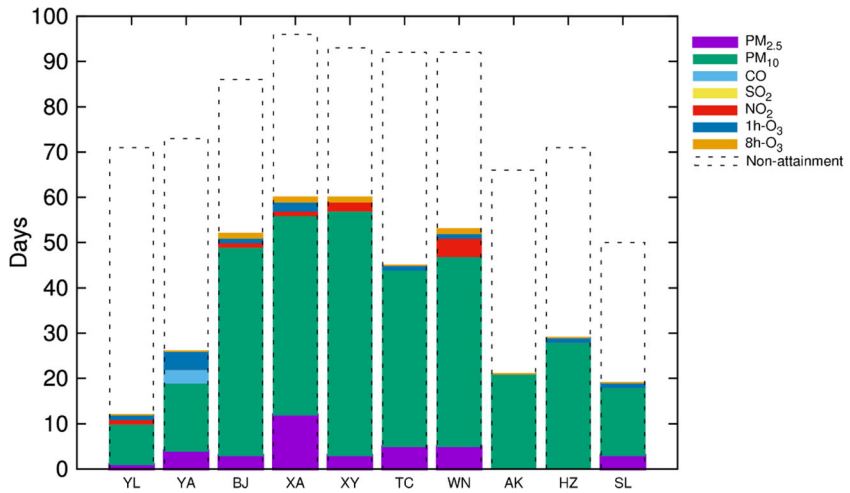

Fig. 5 Number of days when each criteria air pollutant is a nondominant pollutant on nonattainment days

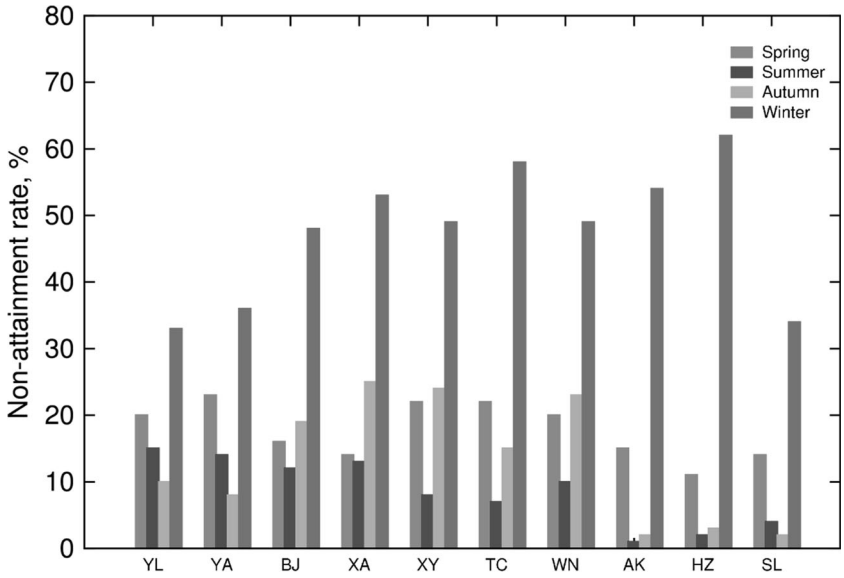

Fig. 6 Seasonal variations in the nonattainment rates

Correspondingly, the intercity relationships for each pollutant may reflect their regional synergy. Thus, we calculated the coefficients of determination (R^2) among the ten cities for the six pollutants both annually and seasonally (Table 4 and Table S3) to assess the possible synergy among pollutants in different terrains.

The correlations among cities in each region were highest for $PM_{2.5}$, PM_{10}, 1 h-O_3, and 8 h-O_3 both annually and seasonally, i.e., cities were significantly correlated ($R^2 \geq 0.5$) in both Guanzhong Plain and the plateau region, except for 1 h- and 8 h-O_3 during the summer in the plateau region, and significantly or moderately correlated ($0.25 \leq R^2 < 0.5$) in the mountain region, except for $PM_{2.5}$ and PM_{10} during the winter when only Ankang and Hanzhong were significantly correlated. For Guanzhong Plain, there were significant correlations for CO during the winter, as well as for SO_2 and NO_2 during the autumn and winter. For the plateau region, cities were significantly correlated for CO and SO_2 during the autumn and for NO_2 during the winter. For the mountain region, cities were moderately correlated for NO_2 during the spring and winter, but weakly correlated ($0 \leq R^2 < 0.25$) for CO and SO_2 in all four seasons.

Table 3 Annual and seasonal frequencies of different criteria air pollutants as the dominant pollutant on nonattainment days

	$PM_{2.5}$	PM_{10}	CO	SO_2	NO_2	1 h-O_3	8 h-O_3
Plateau							
Annual	42.4%	37.5%	0.7%	0.0%	0.7%	0.0%	18.8%
Spring	7.7%	74.4%	2.6%	0.0%	0.0%	0.0%	15.4%
Summer	0.0%	22.2%	0.0%	0.0%	0.0%	0.0%	77.8%
Autumn	62.5%	37.5%	0.0%	0.0%	0.0%	0.0%	0.0%
Winter	77.4%	21.0%	0.0%	0.0%	1.6%	0.0%	0.0%
Plain							
Annual	66.4%	25.5%	0.0%	0.0%	0.0%	0.4%	7.6%
Spring	40.7%	47.7%	0.0%	0.0%	0.0%	0.0%	11.6%
Summer	4.4%	40.0%	0.0%	0.0%	0.0%	4.4%	51.1%
Autumn	68.0%	29.9%	0.0%	0.0%	0.0%	0.0%	2.1%
Winter	87.4%	12.6%	0.0%	0.0%	0.0%	0.0%	0.0%
Mountain							
Annual	83.4%	9.6%	0.0%	0.0%	0.0%	0.5%	6.4%
Spring	54.1%	29.7%	0.0%	0.0%	0.0%	0.0%	16.2%
Summer	0.0%	14.3%	0.0%	0.0%	0.0%	14.3%	71.4%
Autumn	71.4%	14.3%	0.0%	0.0%	0.0%	0.0%	14.3%
Winter	96.3%	3.7%	0.0%	0.0%	0.0%	0.0%	0.0%

The three regions also had moderate correlations in some cases. The plateau region cities were moderately correlated with Guanzhong Plain cities for $PM_{2.5}$ and SO_2 during the autumn and winter, for PM_{10} and CO during the autumn, and for NO_2 and 1 h- and 8 h-O_3 during the spring, autumn, and winter. They were all moderately correlated during the autumn because PBL was high, which facilitated the transportation of air pollutants, and the mountain-plain solenoid circulation usually occurred during the afternoon in the autumn months (May and Wilczak 1993; Sun and Zhang 2012). The mountain region cities were moderately correlated with Guanzhong Plain cities for $PM_{2.5}$ during the autumn, for PM_{10} from the spring to the autumn, for CO during the autumn (except Shangluo), and for NO_2 during the autumn and winter (except Ankang). Besides, there were mostly moderate correlations for 1 h- and 8 h-O_3 in all four seasons.

The back-trajectory analysis was conducted during the most polluted days. For the plateau region, the trajectory showed that the air mass in the two cities mostly from the same direction except in summer, demonstrating their synergy

Table 4 Annual coefficients of determination (R^2) for criteria air pollutants between cities

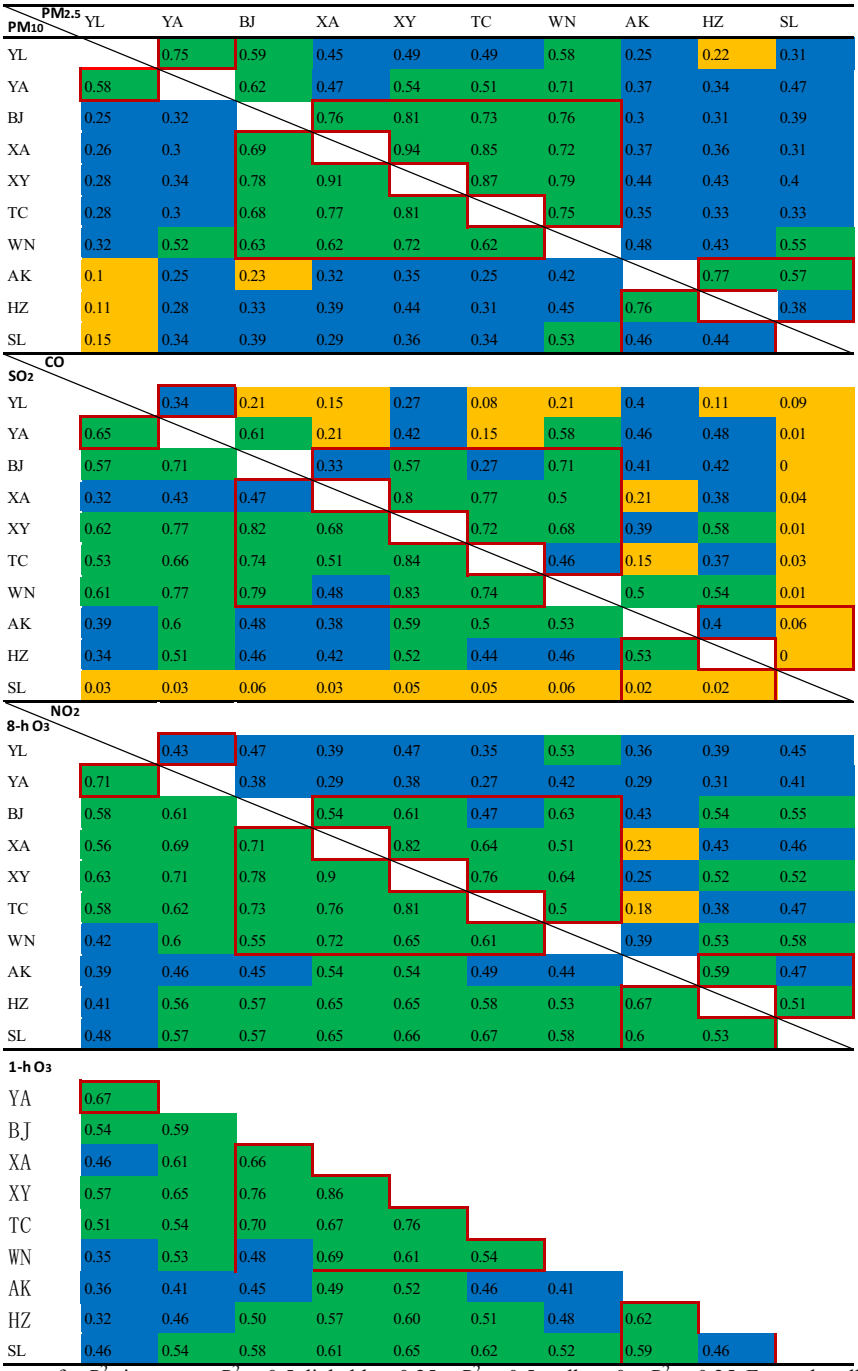

PM_{10} \ $PM_{2.5}$	YL	YA	BJ	XA	XY	TC	WN	AK	HZ	SL
YL		0.75	0.59	0.45	0.49	0.49	0.58	0.25	0.22	0.31
YA	0.58		0.62	0.47	0.54	0.51	0.71	0.37	0.34	0.47
BJ	0.25	0.32		0.76	0.81	0.73	0.76	0.3	0.31	0.39
XA	0.26	0.3	0.69		0.94	0.85	0.72	0.37	0.36	0.31
XY	0.28	0.34	0.78	0.91		0.87	0.79	0.44	0.43	0.4
TC	0.28	0.3	0.68	0.77	0.81		0.75	0.35	0.33	0.33
WN	0.32	0.52	0.63	0.62	0.72	0.62		0.48	0.43	0.55
AK	0.1	0.25	0.23	0.32	0.35	0.25	0.42		0.77	0.57
HZ	0.11	0.28	0.33	0.39	0.44	0.31	0.45	0.76		0.38
SL	0.15	0.34	0.39	0.29	0.36	0.34	0.53	0.46	0.44	

SO_2 \ CO	YL	YA	BJ	XA	XY	TC	WN	AK	HZ	SL
YL		0.34	0.21	0.15	0.27	0.08	0.21	0.4	0.11	0.09
YA	0.65		0.61	0.21	0.42	0.15	0.58	0.46	0.48	0.01
BJ	0.57	0.71		0.33	0.57	0.27	0.71	0.41	0.42	0
XA	0.32	0.43	0.47		0.8	0.77	0.5	0.21	0.38	0.04
XY	0.62	0.77	0.82	0.68		0.72	0.68	0.39	0.58	0.01
TC	0.53	0.66	0.74	0.51	0.84		0.46	0.15	0.37	0.03
WN	0.61	0.77	0.79	0.48	0.83	0.74		0.5	0.54	0.01
AK	0.39	0.6	0.48	0.38	0.59	0.5	0.53		0.4	0.06
HZ	0.34	0.51	0.46	0.42	0.52	0.44	0.46	0.53		0
SL	0.03	0.03	0.06	0.03	0.05	0.05	0.06	0.02	0.02	

8-h O_3 \ NO_2	YL	YA	BJ	XA	XY	TC	WN	AK	HZ	SL
YL		0.43	0.47	0.39	0.47	0.35	0.53	0.36	0.39	0.45
YA	0.71		0.38	0.29	0.38	0.27	0.42	0.29	0.31	0.41
BJ	0.58	0.61		0.54	0.61	0.47	0.63	0.43	0.54	0.55
XA	0.56	0.69	0.71		0.82	0.64	0.51	0.23	0.43	0.46
XY	0.63	0.71	0.78	0.9		0.76	0.64	0.25	0.52	0.52
TC	0.58	0.62	0.73	0.76	0.81		0.5	0.18	0.38	0.47
WN	0.42	0.6	0.55	0.72	0.65	0.61		0.39	0.53	0.58
AK	0.39	0.46	0.45	0.54	0.54	0.49	0.44		0.59	0.47
HZ	0.41	0.56	0.57	0.65	0.65	0.58	0.53	0.67		0.51
SL	0.48	0.57	0.57	0.65	0.66	0.67	0.58	0.6	0.53	

1-h O_3	YA	BJ	XA	XY	TC	WN	AK	HZ	SL
YA		0.67							
BJ	0.54	0.59							
XA	0.46	0.61	0.66						
XY	0.57	0.65	0.76	0.86					
TC	0.51	0.54	0.70	0.67	0.76				
WN	0.35	0.53	0.48	0.69	0.61	0.54			
AK	0.36	0.41	0.45	0.49	0.52	0.46	0.41		
HZ	0.32	0.46	0.50	0.57	0.60	0.51	0.48	0.62	
SL	0.46	0.54	0.58	0.61	0.65	0.62	0.52	0.59	0.46

Colors represent the value range for R^2, i.e., green, $R^2 \geq 0.5$; light blue, $0.25 \leq R^2 < 0.5$; yellow, $0 \leq R^2 < 0.25$. For each pollutant, the three red frames from the upper left corner to the lower right corner show the R^2 values between cities in the plateau region, Guanzhong Plain, and mountain region, respectively

among $PM_{2.5}/PM_{10}$. For Guanzhong Plain, the same most polluted period and similar back-trajectories of the five cities in the same season showed that their air quality were influenced by the similar air mass, and the several short twining trajectories in the plain also indicated their strong synergy for O_3 in summer and $PM_{2.5}$ in other seasons. Furthermore, the air mass from the mountain region indicates their synergy among $PM_{2.5}$. For the mountain region, their back-trajectories were different, i.e., they were short and winding in Ankang and Hanzhong, indicating the strong air mass retention by surrounded mountain. However, some trajectories stretched to northwest, indicating that it was influenced much by other regions, e.g., 8 h-O_3 and $PM_{2.5}$ were moderated with that in Guanzhong Plain in summer and winter, respectively.

Besides, the trajectories in the plateau region and Guanzhong showed that the two regions shared air mass in fall and winter.

Correlations between air pollutants

According to the synergy among pollutants within each region, as discussed above, correlations were also tested among pollutants to investigate their relationships in the three regions (Table 5). We found that there were some common correlations among the three regions. $PM_{2.5}$ was always significantly correlated ($R \geq 0.5$) with PM_{10} in all three regions, possibly because the ratios of $PM_{2.5}$ to PM_{10} were high (0.4–0.8) (Fig. 2), and implied that they may have the same source regions or that they are influenced by the same local conditions (Deshmukh et al. 2013; Rashki et al. 2013). SO_2 and NO_2 were always moderately ($0.25 \leq R < 0.5$) or significantly correlated, thereby suggesting that they had

Table 5 Correlation coefficients (R) between criteria air pollutants in the three regions of Shaanxi

	Plateau						Guanzhong						Mountain					
Yearly	PM_{10}	CO	SO_2	NO_2	1 h-O_3	8 h-O_3	PM_{10}	CO	SO_2	NO_2	1 h-O_3	8 h-O_3	PM_{10}	CO	SO_2	NO_2	1h-O_3	8 h-O_3
$PM_{2.5}$	0.66	0.46	0.56	0.54	-0.3	-0.35	0.9	0.73	0.56	0.68	-0.35	-0.39	0.87	0.5	0.49	0.64	-0.25	-0.3
PM_{10}		0.36	0.37	0.36	-0.16	-0.19		0.67	0.54	0.68	-0.29	-0.32		0.48	0.47	0.6	-0.18	-0.21
CO			0.74	0.49	-0.46	-0.49			0.62	0.63	-0.5	-0.53			0.39	0.6	-0.23	-0.25
SO_2				0.64	-0.49	-0.55				0.56	-0.32	-0.35				0.42	-0.12	-0.13
NO_2					-0.27	-0.36					-0.27	-0.34					-0.37	-0.43
1h-O_3						0.97						0.98						0.98
Spring																		
$PM_{2.5}$	0.65	-0.04	0.28	0.37	0.02	-0.06	0.71	0.5	0.44	0.52	-0.08	-0.14	0.71	0.01	0.24	0.44	0	-0.04
PM_{10}		-0.01	0.18	0.21	-0.06	-0.09		0.34	0.45	0.52	0.07	0.03		0.15	0.26	0.29	0.02	0.04
CO			0.43	-0.06	-0.37	-0.36			0.32	0.33	-0.26	-0.3			0.37	0.1	-0.01	0.01
SO_2				0.36	-0.27	-0.33				0.5	-0.04	-0.06				0.22	0.16	0.15
NO_2					0.26	0.2					0.2	0.13					-0.06	-0.12
1h-O_3						0.97						0.98						0.96
Summer																		
$PM_{2.5}$	0.63	0.32	0.09	0.15	0.14	0.13	0.72	0.33	0.11	0.13	0.08	0.09	0.79	0.34	0.21	0.35	0.34	0.32
PM_{10}		-0.06	0.08	0.21	0.03	-0.01		0.15	0.18	0.38	0.06	0.04		0.31	0.24	0.42	0.33	0.3
CO			-0.09	0.39	0.06	-0.01			0.02	0.12	0.09	0.05			0.03	0.7	0.09	0.07
SO_2				0.26	0.24	0.16				0.37	0.3	0.29				0.24	0.18	0.2
NO_2					0.24	0.16					0.28	0.21					0.12	0.09
1h-O_3						0.93						0.98						0.95
Autumn																		
$PM_{2.5}$	0.69	0.57	0.39	0.45	-0.11	-0.17	0.88	0.63	0.41	0.61	0.02	-0.02	0.87	0.13	0.21	0.32	0.24	0.2
PM_{10}		0.3	0.34	0.55	0.08	-0.02		0.54	0.41	0.61	0.03	-0.01		0.09	0.14	0.29	0.22	0.19
CO			0.7	0.64	-0.56	-0.63			0.58	0.55	-0.42	-0.45			0.19	0.47	0.14	0.15
SO_2				0.56	-0.41	-0.48				0.65	-0.15	-0.2				0.13	0.11	0.12
NO_2					-0.21	-0.34					0.01	-0.08					-0.14	-0.18
1h-O_3						0.97						0.99						0.98
Winter																		
$PM_{2.5}$	0.66	0.35	0.38	0.5	-0.12	-0.22	0.94	0.67	0.37	0.75	-0.44	-0.49	0.88	0.66	0.45	0.58	-0.24	-0.34
PM_{10}		0.26	0.25	0.18	0.11	0.07		0.69	0.33	0.73	-0.42	-0.47		0.61	0.49	0.62	-0.13	-0.23
CO			0.73	0.51	-0.04	-0.19			0.38	0.65	-0.35	-0.4			0.36	0.64	-0.33	-0.45
SO_2				0.66	-0.02	-0.27				0.46	-0.07	-0.13				0.37	-0.12	-0.17
NO_2					-0.21	-0.5					-0.43	-0.54					-0.26	-0.44
1h O_3						0.89						0.96						0.95

Colors represent the value ranges for R, i.e., green, $R \geq 0.5$; light blue, $0.25 \leq R < 0.5$; yellow, $-0.25 \leq R < 0.25$; red, $R < -0.25$

common sources (e.g., fossil fuels) and elimination reactions (e.g., secondary inorganic aerosol (SIA) formation). NO_2 and SO_2 always had positive correlations with $PM_{2.5}$ and PM_{10}, where the correlation with $PM_{2.5}$ (significant or moderate) was better than that with PM_{10} (moderate or weak ($0 < R < 0.25$)). This is mainly because sulfate and nitrate, which are emitted directly together with NO_2 and SO_2, or as SIA generated via gas-phase oxidation or aqueous reactions from the two species, have important effects on $PM_{2.5}$ (Ervens et al. 2011; Fang et al. 2009; Guo et al. 2014; Huang et al. 2014). In addition, the difference between the two correlations may be explained by the contribution of nitrate exceeding that of sulfate in SIA.

There were seasonal and spatial variations in the other correlations (i.e., 8 h-O_3 with other species, and CO with $PM_{2.5}$, PM_{10}, SO_2, and NO_2). We found that 8 h-O_3 had the most significant negative correlations ($R < -0.25$) with other pollutants during the winter in all three regions, possibly because the meteorological conditions were conducive to the accumulation of the other five pollutants, but not for 8 h-O_3 because the solar radiation level was lower with high aerosol pollution. NO_2 had a negative correlation with 8 h-O_3. During the summer, 8 h-O_3 was significantly correlated with $PM_{2.5}$ and PM_{10} only in the mountain region, thereby indicating that the simultaneous formation of secondary O_3 and $PM_{2.5}$ via photochemical reactions (Sakulyanontvittaya et al. 2009; Ying et al. 2015) was greater than that in the other two regions. During the spring and autumn, 8 h-O_3 had significant negative correlations with CO and SO_2 in the plateau region, where the main difference was that 8 h-O_3 was weakly correlated with NO_2 during the spring but significantly negatively correlated during the autumn. During the spring and autumn, 8 h-O_3 was also significantly correlated with CO in Guanzhong Plain, whereas the other correlations (i.e., 8 h-O_3 with $PM_{2.5}$, PM_{10}, SO_2, and NO_2) were weak. The correlations were weak ($-0.25 \le R < 0.25$) in the mountain region during the two seasons.

There were significant or moderate correlations between CO with $PM_{2.5}$, PM_{10}, SO_2, and NO_2, during the winter in all three regions, thereby suggesting that their common origin was fossil fuel combustion. During the autumn, their correlations were similar to those during the winter in the plateau region and Guanzhong Plain, whereas the correlations were weak in the mountain region, except for a moderate correlation with NO_2, which indicates that less coal was burned in the mountain region, and thus, the CO and NO_2 concentrations were influenced greatly by vehicles. During the spring, there were moderate correlations in Guanzhong Plain but CO was only moderately correlated with SO_2 in the other two regions. CO was also moderately correlated with $PM_{2.5}$ and NO_2 in the plateau region during the summer, but only moderately correlated with $PM_{2.5}$ and weakly correlated with NO_2 in Guanzhong Plain. 1 h-O_3 was much significantly correlated with 8 h-O_3 and their correlation with other pollutants was similar.

Comparison among cities

To further assess the terrain effects on air pollution, comparisons among three cities with similar population (Yulin, Baoji, and Hanzhong) were conducted in the three corresponding terrain regions. The concentrations of most pollutants in Baoji were usually higher than Hanzhong and Yulin (Fig. 2). The concentrations of most pollutants such as $PM_{2.5}$ and PM_{10} in Baoji are usually higher than those in Hanzhong and Yulin especially in the winter, as the plain terrain was easy for air pollutants emitted from Xi'an, Xianyang, and Weinan, which had much more population than Baoji, to reach Baoji. Loess Plateau is arid and much of its surface is exposed, so PM_{10} is relatively high in Yulin in spring. The PM_{10} level in Yulin was close to that in Baoji and was slightly higher than that in Hanzhong from spring to autumn. Besides, the relative high altitude may made the region receive stronger solar radiation and have longer sunshine hours, leading to high 1 h- and 8 h-O_3 in all seasons. The mountain region can retain pollutants by surrounding mountains especially in winter. The concentrations of $PM_{2.5}$ and PM_{10} in Hanzhong increased to approximate to those of Baoji in winter.

$PM_{2.5}$, PM_{10}, and 8 h-O_3 were the three most frequent dominant pollutants in Yulin. $PM_{2.5}$ was the most frequent dominant pollutant in Baoji, and PM_{10} appeared as dominant pollutant in all seasons. $PM_{2.5}$ also was the most frequent pollutant in Hanzhong, but PM_{10} was the dominant pollutant only in spring (Table S4). The correlation coefficients of the five pollutants (except 8 h-O_3) were lowest in Yulin, especially in summer (Table S5), indicating that there was complex relationship in plateau region. $PM_{2.5}$ showed significant correlation with PM_{10} in the three cities, and the correlation was always highest in Hanzhong, indicating the close relationship between $PM_{2.5}$ and PM_{10}.

Conclusion

In this study, the characteristics of six criteria pollutants were analyzed in the three terrain regions in Shaanxi in 2015. Shaanxi was mainly affected by 8 h-O_3 during the summer and by $PM_{2.5}$ and PM_{10} in the other seasons. The high concentrations of the pollutants (except 8 h-O_3) and the number of nonattainment days showed that the air quality was poorest during the winter, especially in the Guanzhong Plain and mountain regions. Cities in the three regions were mostly significantly correlated for $PM_{2.5}$, PM_{10}, and 8 h-O_3, especially in Guanzhong Plain, which suggests that the location of cities in plains surrounded by mountains can readily lead to synergy

among pollutants with high concentrations. The moderate correlations among the three regions for some pollutants showed that synergy among pollutants also occurred on a large scale in some cases. In addition, nonattainment days in the mountain region were rare during the summer and autumn, but they increased greatly during the winter when $PM_{2.5}$ was the dominant pollutant, showing the special polluted characteristics in the mountain region in winter. These results provide insights into the combined influence of air pollution from regional cities, and they may also help governors of different cities to understand the importance of working together to reduce air pollution.

Future studies should focus on the effects and contributions of extra-regional transport of pollutants to obtain a more comprehensive understanding of air pollution in Shaanxi. The local sources, the transport of pollutants, and chemical compositions of $PM_{2.5}$ in the synergistic pollution-affected region during highly polluted seasons should also be investigated to elucidate the mechanisms responsible for the formation of air pollution and to design effective control strategies.

Funding information This study is supported by the National 12th Five-Year Scientific and Technological Support Plan (Grant #2015BAD07B06), and the "948" project from the State Forestry Administration of China (grant #2013–4–56).

References

Cheng W-L, Chen Y-S, Zhang J, Lyons T, Pai J-L, Chang S-H (2007) Comparison of the revised air quality index with the PSI and AQI indices. Sci Total Environ 382:191–198

Deshmukh DK, Deb MK, Mkoma SL (2013) Size distribution and seasonal variation of size-segregated particulate matter in the ambient air of Raipur city, India. Air Qual Atmos Health 6:259–276

Ervens B, Turpin BJ, Weber RJ (2011) Secondary organic aerosol formation in cloud droplets and aqueous particles (aqSOA): a review of laboratory, field and model studies. Atmos Chem Phys 11:11069–11102

Fang M, Chan CK, Yao X (2009) Managing air quality in a rapidly developing nation: China. Atmos Environ 43:79–86

Gao Y, Liu X, Zhao C, Zhang M (2011) Emission controls versus meteorological conditions in determining aerosol concentrations in Beijing during the 2008 Olympic Games. Atmos Chem Phys 11: 12437–12451

Guo S, Hu M, Zamora ML, Peng J, Shang D, Zheng J, Du Z, Wu Z, Shao M, Zeng L, Molina MJ, Zhang R (2014) Elucidating severe urban haze formation in China. Proc Natl Acad Sci U S A 111:17373–17378

Gurjar BR, Butler TM, Lawrence MG, Lelieveld J (2008) Evaluation of emissions and air quality in megacities. Atmos Environ 42:1593–1606

Hu J, Wang Y, Ying Q, Zhang H (2014) Spatial and temporal variability of PM2.5 and PM10 over the North China Plain and the Yangtze River Delta, China. Atmos Environ 95:598–609

Hu J, Ying Q, Wang Y, Zhang H (2015) Characterizing multi-pollutant air pollution in China: comparison of three air quality indices. Environ Int 84:17–25

Huang RJ, Zhang Y, Bozzetti C, Ho KF, Cao JJ, Han Y, Daellenbach KR, Slowik JG, Platt SM, Canonaco F, Zotter P, Wolf R, Pieber SM, Bruns EA, Crippa M, Ciarelli G, Piazzalunga A, Schwikowski M, Abbaszade G, Schnelle-Kreis J, Zimmermann R, An Z, Szidat S, Baltensperger U, El Haddad I, Prevot AS (2014) High secondary aerosol contribution to particulate pollution during haze events in China. Nature 514:218–222

Jazcilevich AD, García AR, Caetano E (2005) Locally induced surface air confluence by complex terrain and its effects on air pollution in the valley of Mexico. Atmos Environ 39:5481–5489

Ji D, Wang Y, Wang L, Chen L, Hu B, Tang G, Xin J, Song T, Wen T, Sun Y, Pan Y, Liu Z (2012) Analysis of heavy pollution episodes in selected cities of northern China. Atmos Environ 50:338–348

Lei W, De Foy B, Zavala M, Volkamer R, Molina LT (2007) Characterizing ozone production in the Mexico City Metropolitan area, a case study using a chemical transport model. Atmos Chem Phys 7:1347–1366

May PT, Wilczak JM (1993) Diurnal and seasonal-variations of boundary-layer structure observed with a radar wind profiler and rass. Mon Weather Rev 121:673–682

Qu WJ, Arimoto R, Zhang XY, Zhao CH, Wang YQ, Sheng LF, Fu G (2010) Spatial distribution and interannual variation of surface PM_{10} concentrations over eighty-six Chinese cities. Atmos Chem Phys 10: 5641–5662

Quan J, Tie X, Zhang Q, Liu Q, Li X, Gao Y, Zhao D (2014) Characteristics of heavy aerosol pollution during the 2012–2013 winter in Beijing, China. Atmos Environ 88:83–89

Querol X, Alastuey A, Pandolfi M, Reche C, Pérez N, Minguillón MC, Moreno T, Viana M, Escudero M, Orio A (2014) 2001–2012 trends on air quality in Spain. Sci Total Environ 490:957–969

Rashki A, CJd R, Eriksson PG, Kaskaoutis DG, Gupta P (2013) Temporal changes of particulate concentration in the ambient air over the city of Zahedan, Iran. Air Qual Atmos Health 6:123–135

Rolph G, Stein A, Stunder B (2017) Real-time Environmental Applications and Display sYstem: READY. Environ Model Softw 95:210–228

Sakulyanontvittaya T, Guenther A, Helmig D, Milford J, Wiedinmyer C (2009) Secondary organic aerosol from sesquiterpene and monoterpene emissions in the United States. Environ Sci Technol 42:8784–8790

Santurtún A, González-Hidalgo JC, Sanchez-Lorenzo A, Zarrabeitia MT (2015) Surface ozone concentration trends and its relationship with weather types in Spain (2001–2010). Atmos Environ 101:10–22

Sun J, Zhang F (2012) Impacts of mountain-plains solenoid on diurnal variations of rainfalls along the Mei-Yu front over the East China Plains. Mon Weather Rev 140:379–397

Tie X, Madronich S, Li G, Ying Z, Zhang R, Garcia AR, Lee-Taylor J, Liu Y (2007) Characterizations of chemical oxidants in Mexico City: a regional chemical dynamical model (WRF-Chem) study. Atmos Environ 41:1989–2008

Wang D, Hu J, Xu Y, Lv D, Xie X, Kleeman M, Xing J, Zhang H, Ying Q (2014a) Source contributions to primary and secondary inorganic particulate matter during a severe wintertime PM2.5 pollution episode in Xi'an, China. Atmos Environ 97:182–194

Wang Y, Li L, Chen C, Huang C, Huang H, Feng J, Wang S, Wang H, Zhang G, Zhou M, Cheng P, Wu M, Sheng G, Fu J, Hu Y, Russell AG, Wumaer A (2014b) Source apportionment of fine particulate matter during autumn haze episodes in Shanghai, China. J Geophys Res: Atmos 119:1903–1914

Wang Y, Ying Q, Hu J, Zhang H (2014c) Spatial and temporal variations of six criteria air pollutants in 31 provincial capital cities in China during 2013-2014. Environ Int 73:413–422

Xu Y, Hu J, Ying Q, Hao H, Wang D, Zhang H (2017) Current and future emissions of primary pollutants from coal-fired power plants in Shaanxi, China. Sci Total Environ 595:505–514

Yang F, Tan J, Zhao Q, Du Z, He K, Ma Y, Duan F, Chen G, Zhao Q (2011) Characteristics of $PM_{2.5}$ speciation in representative megacities and across China. Atmos Chem Phys 11:5207–5219

Yerramilli A, Dodla VBR, Challa VS, Myles L, Pendergrass WR, Vogel CA, Dasari HP, Tuluri F, Baham JM, Hughes RL, Patrick C, Young JH, Swanier SJ, Hardy MG (2012) An integrated WRF/HYSPLIT modeling approach for the assessment of PM2.5 source regions over the Mississippi Gulf Coast region. Air Qual Atmos Health 5:401–412

Ying Q, Li J, Kota SH (2015) Significant contributions of isoprene to summertime secondary organic aerosol in eastern United States. Environ Sci Technol 49:7834–7842

Zhang J, Zhang L-y DM, Zhang W, Huang X, Zhang Y-q, Yang Y-y, Zhang J-m, Deng S-h, Shen F, Li Y-w, Xiao H (2016) Indentifying the major air pollutants base on factor and cluster analysis, a case study in 74 Chinese cities. Atmos Environ 144:37–46

Zhang R, Lei W, Tie X, Hess P (2004) Industrial emissions cause extreme diurnal urban ozone variability. Proc Natl Acad Sci U S A 101: 6346–6350

Zhang XY, Cao JJ, Li LM, Arimoto R, Cheng Y, Huebert B, Wang D (2002) Characterization of atmospheric aerosol over XiAn in the south margin of the loess plateau, China. Atmos Environ 36:4189–4199

Zhang YL, Cao F (2015) Fine particulate matter (PM 2.5) in China at a city level. Sci Rep 5:14884

Zhao P, Feng Y, Zhu T, Wu J (2006) Characterizations of resuspended dust in six cities of North China. Atmos Environ 40:5807–5814

Zhao S, Yu Y, Yin D, He J, Liu N, Qu J, Xiao J (2016) Annual and diurnal variations of gaseous and particulate pollutants in 31 provincial capital cities based on in situ air quality monitoring data from China National Environmental Monitoring Center. Environ Int 86:92–106

Zhu Y, Zhang J, Wang J, Chen W, Han Y, Ye C, Li Y, Liu J, Zeng L, Wu Y (2016) Distribution and sources of air pollutants in the North China Plain based on on-road mobile measurements. Atmos Chem Phys 16:12551–12565